Available online at www.sciencedirect.com

ScienceDirect

Mendeleev Commun., 2023, **33**, 653–656

Mendeleev Communications

Molecular structure of 3,3-pentamethylenediaziridine in gas and solution phases

Alexander V. Belyakov,[a] Vladimir V. Kuznetsov,[b] Nadezhda S. Kormil'tsina,[a] Galina S. Shimanskaya,[a] Anatoly N. Rykov,[c] Andrey S. Dmitrenok,[b] Yulia V. Novakovskaya[c] and Igor F. Shishkov*[c]

[a] *St. Petersburg State Institute of Technology (Technical University), 190013 St. Petersburg, Russian Federation*
[b] *N. D. Zelinsky Institute of Organic Chemistry, Russian Academy of Sciences, 119991 Moscow, Russian Federation*
[c] *Department of Chemistry, M. V. Lomonosov Moscow State University, 119991 Moscow, Russian Federation. E-mail: ifshishkov@phys.chem.msu.ru*

DOI: 10.1016/j.mencom.2023.09.021

The equilibrium molecular structure of the 3,3-pentamethylenediaziridine (PMDA) molecule in the gas phase was determined by gas-phase electron diffraction in combination with quantum chemical calculations up to the CCSD(T)-AE/cc-pwCVQZ level and estimation of the mean amplitudes and anharmonic vibrational corrections using quadratic and cubic force fields. 1D and 2D ^{1}H and ^{13}C NMR spectra of PMDA in a $CDCl_3$ solution recorded at different temperatures revealed the temperature dependence of the chemical shifts of NH protons. Nonempirical simulations of small PMDA clusters, carried out at the DFT-B3LYP/6-31++G(2d,p) level, enabled us to suggest an interpretation of the NMR data.

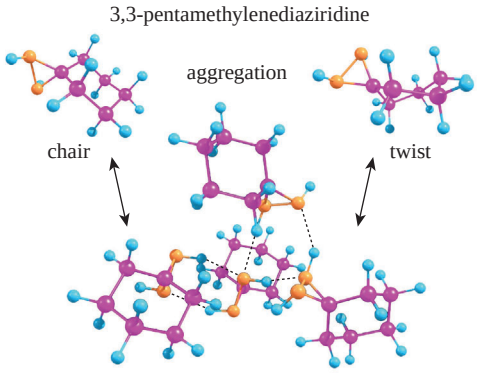

Keywords: 3,3-pentamethylenediaziridine, gas-phase electron diffraction, GED, molecular structure, NMR spectra, PMDA clusters.

Derivatives of diaziridine (diazacyclopropane) have a pronounced effect on the central nervous system, exhibiting various types of neurotropic activity.[1–3] To date, a number of studies have identified the antidepressant effects of 1-[2-(3,3-dimethyldiaziridin-1-yl)ethyl]-3,3-dimethyldiaziridine, known as tetramezine.[4,5] An important field of modern medicinal chemistry is the design of drugs based on the combination of several pharmacologically active fragments in one molecule.[6,7] One of these fragments can be cyclohexane, which nowadays plays a significant role in pharmacology.[8] A number of compounds of the cyclohexane family have been successfully tested as antianginal, hypoglycemic and anticonvulsant drugs, as well as drugs used in the treatment of Parkinson's disease and epilepsy. Some drugs based on cyclohexane, such as Validol, Gabapentin, Cyclamide and Amedin, are used in medical practice. In this work, a structural analysis of 3,3-pentamethylenediaziridine (PMDA) was carried out, which involves both diaziridine and cyclohexane fragments and serves as the basis for a drug with a confirmed high anxiolytic activity.[1] Insofar as different conformations of a molecule can produce different effects and differ in different phases, the investigation of the structure of PMDA in both gas and condensed phases by gas-phase electron diffraction (GED) and NMR techniques in combination with nonempirical simulations is of high demand.

The synthesis and characterization of PMDA was carried out according to the techniques outlined in Online Supplementary Materials. The structure of an individual PMDA molecule in the gas phase was found based on a combination of GED data (Table S1, see Online Supplementary Materials) and quantum chemical simulations. To obtain relative differences in structural parameters in terms of the known additive scheme,[9–16] geometry optimization was carried out at the CCSD(T)-FC level with the cc-pVTZ (hereinafter VTZ) basis set. The composite parameters of the best theoretical equilibrium (BTE) structure of the PMDA molecule were then calculated as follows:

$$r_e[\text{CCSD(T)-AE/wCVQZ}] = r_e[\text{CCSD(T)-FC/VTZ}] + \{r_e(\text{MP2-AE/wCVTZ}) - r_e(\text{MP2-FC/wCVTZ})\} + \{r_e(\text{MP2-FC/VQZ}) - r_e(\text{MP2-FC/VTZ})\}, \quad (1)$$

where AE and FC denote the all-electron and frozen-core calculations, respectively (Table S2). The accuracy of this method, based on the additivity of small relative differences in structural parameters, has been repeatedly confirmed.[9–17] The normal-coordinate analysis proved that the structures with point-group symmetry C_1 correspond to the minima of the potential energy surface (PES). MP2 and DFT calculations were carried out using the Gaussian 16 (Revision C.01) program,[18] and CCSD(T) calculations were performed using the CFOUR program.[19] The mean amplitudes ($u_{ij,h1}$) and vibrational corrections ($r_{ij,e} - r_{ij,a}$) given in Table S3, required for GED data analysis, were computed using quadratic and cubic force fields in first-order perturbation theory, taking into account nonlinear kinematic effects using the SHRINK program.[20–23] Quadratic and cubic force fields were calculated using the B2PLYP functional and the VTZ basis set.

To refine the structural parameters, the following functional of the form

$$Q = \sum_s w_s \Delta_s^2 = \sum_s w_s [sM^{\text{obs}}(s) - ksM^{\text{calc}}(s)]^2, \quad (2)$$

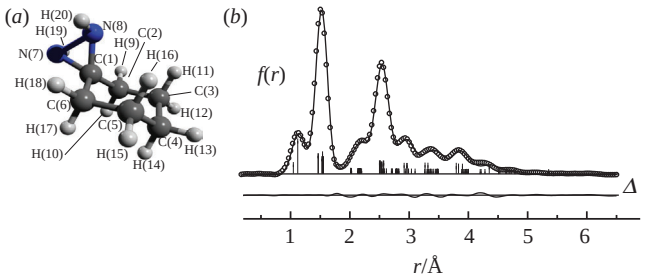

Figure 1 (*a*) Structure of a PMDA molecule with atom numbering. (*b*) Experimental (○) and calculated (–) radial distribution functions $f(r)$ of PMDA and their difference (Δ) estimated by subtracting the theoretical values from the experimental ones.

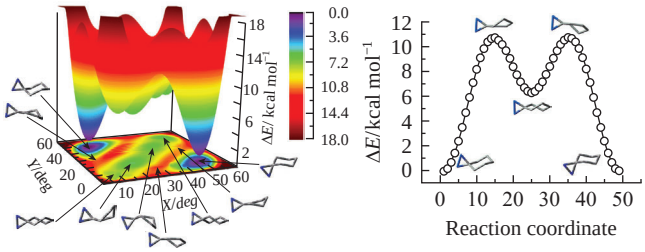

Figure 2 (*a*) 2D and (*b*) 1D cross-sections of the PES of PMDA along the coordinates of dihedral angles C(1)–C(2)–C(3)–C(4) (*X*) and C(1)–C(6)–C(5)–C(4) (*Y*), corresponding to the chair–twist–chair transformation.

in which $sM(s)$ is a function of molecular intensity, $s = (4\pi/\lambda)\sin(\theta/2)$ with θ and λ denoting the scattering angle and wavelength of the electron beam, respectively, w_s is the weight function and k is the scale factor, was minimized using the *R*-factor as a criterion. Structure refinement by the least squares method was performed using a modified version of the KCED25 program.[24] The weight matrices were diagonal. GED camera distance data were taken with weights of 0.5 and 1.0 for short and long camera distance, respectively.

Molecular structure of PMDA [Figure 1(*a*)] is determined by 11 internuclear distances, 19 bond angles and 20 dihedral angles, among which one distance, three bond angles and four dihedral angles are the ring closure parameters. Geometric parameters and mean least-squares vibrational amplitudes were refined in groups with constant differences, starting with theoretical BTE and DFT-B2PLYP values, respectively.

In particular, the mean least-squares amplitudes were refined in six groups according to specific ranges of the radial distribution curve [Figure 1(*b*)]: 1.0−1.9, 1.9−2.3, 2.3−2.8, 2.8−3.1, 3.1−3.6, 3.6−4.1 and 4.1–6.0 Å. The internuclear distances were refined in two groups, namely, the C/N–H and all other distances. The bond angles were set equal to the theoretical BTE values. The resulting structural parameters of the lowest energy chair conformer of the molecule are listed in Tables 1 and S5, and the correlation between the refined parameters is given in Table S4.

Table 1 Main equilibrium structural parameters of the chair conformer of the PMDA molecule.

Bond	d/Å[a]	Bond angles	∠/deg	Dihedral angles	∠/deg
C(1)–C(2)	1.505	C(1)–C(2)–C(3)	110.1	C(1)–C(2)–C(3)–C(4)	54.4
C(2)–C(3)	1.528	C(2)–C(3)–C(4)	111.1	C(2)–C(3)–C(4)–C(5)	–56.6
C(3)–C(4)	1.526	C(3)–C(4)–C(5)	111.0	C(3)–C(4)–C(5)–C(6)	56.7
C(4)–C(5)	1.526	C(4)–C(5)–C(6)[b]	110.7	C(1)–C(6)–C(5)–C(4)	–54.8
C(5)–C(6)	1.527	C(1)–C(6)–C(5)[b]	110.3	C(2)–C(1)–C(6)–C(5)[b]	55.0
C(1)–C(6)	1.505	C(2)–C(1)–C(6)[b]	114.2	C(3)–C(2)–C(1)–C(6)[b]	–54.7
C(1)–N(7)	1.440	C(2)–C(1)–N(7)	120.5	C(3)–C(2)–C(1)–N(7)	160.1
N(7)–N(8)	1.511	C(3)–C(2)–H(9)	110.9	C(2)–C(1)–N(7)–N(8)	–104.0
C(1)–N(8)[b]	1.446	C(3)–C(2)–H(10)	109.8	C(4)–C(3)–C(2)–H(9)	175.1
$(C–H)_{av}$	1.121	C(4)–C(3)–H(11)	109.3	C(4)–C(3)–C(2)–H(10)	–65.5
$(N–H)_{av}$	1.047	C(4)–C(3)–H(12)	110.5	C(5)–C(4)–C(3)–H(11)	63.2
		C(5)–C(4)–H(13)	110.2	C(5)–C(4)–C(3)–H(12)	–179.1
		C(5)–C(4)–H(14)	109.1	C(6)–C(5)–C(4)–H(13)	179.0
		C(6)–C(5)–H(15)	110.1	C(6)–C(5)–C(4)–H(14)	–63.8
		C(6)–C(5)–H(16)	109.3	C(1)–C(6)–C(5)–H(15)	–177.4
		C(1)–C(6)–H(17)	108.5	C(1)–C(6)–C(5)–H(16)	65.4
		C(1)–C(6)–H(18)	109.2	C(2)–C(1)–C(6)–H(17)	–65.0
		C(1)–N(7)–H(19)	108.3	C(2)–C(1)–C(6)–H(18)	178.4
		C(1)–N(8)–H(20)	108.3	C(2)–C(1)–N(7)–H(19)	–9.5
				C(2)–C(1)–N(8)–H(20)	–152.6

[a] The *R*-factor is 5.0%. For the two groups of refined internuclear distances (see text), the standard deviations 3σ of LS refinement is 0.006 Å. The numbering of atoms is shown in Figure 1(*a*). [b] Ring closure parameters.

To clarify the reasons why only one conformer was detected in GED experiments, despite the expected possible variations in ring geometry, the PES cross-sections of the PMDA molecule were constructed at the DFT level with the B3LYP hybrid exchange-correlation functional and the 6-31++G(2d,p) basis set. Figure 2(*a*) shows a two-dimensional cross-section of the PES, which corresponds to variations in two opposite dihedral angles of the ring. The chair conformers correspond to position coordinates in the upper left and lower right corners. The path with the lowest energy between the chair conformers is shown in Figure 2(*b*) and corresponds to the transformation of the first chair form through the half-chair transition state (TS) into the twist form located in the lower left corner in Figure 2(*a*) and then, through the second half-chair transition state, to the second chair conformer. For symmetry reasons, there is a mirror path that includes another twist form, located in the upper right corner in Figure 2(*a*). The path was calculated using the quadratic synchronous transit method, STQN.[25,26] As can be seen, the difference in energy between the two conformers is about 6 kcal mol^{-1}, and the barrier on the path is above 10 kcal mol^{-1}, which explains the actual presence of only the chair conformer in the gas phase.

At the same time, NMR experiments (for details, see Online Supplementary Materials) revealed an interesting peculiarity of PMDA in $CDCl_3$ solution. ^{1}H NMR spectra were recorded at several temperatures, and as the temperature changed, a noticeable upfield shift in the signals of N-bonded H(19) and H(20) protons was observed. This shift occured from 1.536 ppm at 298 K to 1.533 ppm at 302 K and further to 1.484 ppm at 323 K with a simultaneous change in the signal shape (Figures S3, S4, S6 and S7, see Online Supplementary Materials). The ^{1}H chemical shift is a sensitive parameter associated with both conformational changes in molecules and changes caused by intermolecular interactions, accompanied by a change in the electron density distribution around particular nuclei. Taking into account that PMDA molecules form continuous sequences of H-bonds in the crystal structure,[27] aggregation due to the formation of H-bonds is quite possible in the liquid phase as well. Therefore, the temperature-dependent changes mentioned above may be due to both factors.

To elucidate the nature of intermolecular interactions of PMDA molecules, a series of quantum chemical simulations of small PMDA clusters at the DFT-B3LYP/6-31++G(d,p) level was carried out using the Firefly program package,[28] and the results were visualized using the Chemcraft software.[29] Only structures with the lowest energy among those identified in optimization runs are considered below. The stability of the clusters was judged on the basis of estimates of the vertical (DE_v) and adiabatic (DE_{ad}) dissociation energies obtained as follows:

$$DE_{ad} = nE(\text{PMDA}) - E(\text{PMDA}_n) + \frac{1}{2}\text{BSSE},$$

$$DE_v = \sum_{k=1}^{n} E'_k(\text{PMDA}) - E(\text{PMDA}_n) + \frac{1}{2}\text{BSSE},$$

where $E(PMDA_n)$ and $E(PMDA)$ are the total adiabatic energies of the $PMDA_n$ cluster and the PMDA monomer in their optimal configurations, respectively, $E'_k(PMDA)$ is the energy of the *k*-th monomer in its configuration in the corresponding cluster, and BSSE is the standard basis set superposition error.

Molecules that oppose each other in two adjacent sequences of hydrogen bonds in the crystal structure,[27] when considered as an individual dimer, can readily form a closed H-bonded ring [Figure 3(*a*)]. Such double N–H···N bridges between two molecules, along with sequences of N–H···N bonds connecting several molecules into structural rings, are also present in larger clusters [Figure 3(*b*)–(*d*)]. The estimated values DE_{ad} and DE_v of the dissociation energy of small clusters (Table 2) show that the bonds themselves are relatively strong, namely, the mean H-bond energy is at least 5.6–5.8 kcal mol^{-1} and increases with the number of molecules in the cluster, or in other words, with an increase in the number of H-bonds, combined into continuous sequences. Such energies are high enough to ensure the aggregation of molecules in a $CDCl_3$ solution. At the same time, the vertical and adiabatic energies are very close, which means that the perturbation of individual molecules upon such aggregation is not as substantial. Furthermore, the energies themselves are comparable to or even slightly higher than the energy difference between the two conformers (chair and twist) of PMDA. Such closeness of energy characteristics shows that for a conformational change of a certain molecule, approximately the same energy is sufficient that is released during the formation of a hydrogen bond. Since both processes can be closely localized and, therefore, proceed simultaneously, there may be a certain conjugation between them.

The conformational transformation can be facilitated to a certain extent by an increase in temperature due to the activation of low-frequency distortion and twisting vibrations. Taking into account that aggregation is driven by hydrophilic interactions, and pentamethylene fragments of molecules form an outer coating of the central H-bonded part of cluster structures, it is quite possible that conformational transformations inside the fragments can proceed without noticeable perturbation of the next neighboring intermolecular contacts. The latter may affect only relatively weak dispersion interactions between methylene groups belonging to the same or different neighboring molecules. If we additionally take into account the relative weakening of H-bonds with increasing temperature, then it easily follows that both processes can contribute to the observed temperature dependences of the chemical shifts of NH protons.

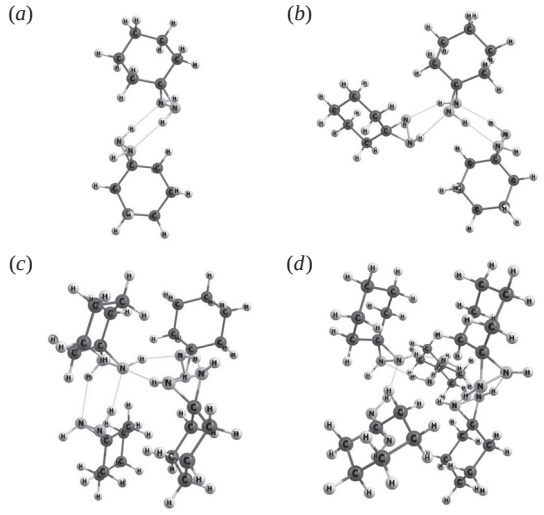

Figure 3 Structures of lowest energy PMDA clusters: (*a*) dimer, (*b*) trimer, (*c*) tetramer and (*d*) pentamer.

Table 2 Vertical (DE_v) and adiabatic (DE_{ad}) dissociation energies of $PMDA_n$ clusters and the number ($N_{H\text{-bond}}$) of hydrogen bonds stabilizing the clusters.

n in $PMDA_n$	DE_v/kcal mol^{-1}	DE_{ad}/kcal mol^{-1}	$N_{H\text{-bond}}$
2	11.2	11.1	2
3	23.3	22.7	4
4	35.1	34.1	5
5	49.9	49.1	7

Thus, 3,3-pentamethylenediaziridine molecule, whose equilibrium structure parameters in the gas phase were determined on the basis of GED data, is a very interesting particle, since the energy difference between its chair and twist conformations nearly coincides with the mean energy of hydrogen bonds between molecules in their clusters. On the one hand, the peculiarities of H-bonding qualitatively account for the temperature dependence of the NMR chemical shifts of NH protons. On the other hand, the closeness of energies indicated above, along with a minor perturbation of the hydrophobic parts of molecules upon their aggregation, can make the chair–twist conformational transformation, which does not occur in the gas phase, quite possible in a liquid. This interesting aspect deserves special attention and will be studied in more detail in the near future.

Online Supplementary Materials

Supplementary data associated with this article can be found in the online version at doi: 10.1016/j.mencom.2023.09.021.

References

1 N. N. Makhova, V. Y. Petukhova, A. V. Shevtsov, V. V. Novakovskiy and V. V. Kuznetsov, *WO Patent 2013/121334 A2*, 2013.
2 V. V. Kuznetsov, A. V. Shevtsov, M. I. Pleshchev, Yu. A. Strelenko and N. N. Makhova, *Mendeleev Commun.*, 2016, **26**, 391.
3 A. V. Belyakov, V. V. Kuznetsov, G. S. Shimanskaya, A. N. Rykov, A. S. Goloveshkin, Yu. V. Novakovskaya and I. F. Shishkov, *Mendeleev Commun.*, 2023, **33**, 95.
4 M. Kamuf and O. Trapp, *Chirality*, 2011, **23**, 113.
5 L. S. Khaikin, I. V. Kochikov, A. N. Rykov, O. E. Grikina, G. G. Ageev, I. F. Shishkov, V. V. Kuznetsov and N. N. Makhova, *Phys. Chem. Chem. Phys.*, 2019, **21**, 5598.
6 E. Borretto, L. Lazzarato, F. Spallotta, C. Cencioni, Y. D'Alessandra, C. Gaetano, R. Fruttero and A. Gasco, *ACS Med. Chem. Lett.*, 2013, **4**, 994.
7 V. P. Ananikov, E. A. Khokhlova, M. P. Egorov, A. M. Sakharov, S. G. Zlotin, A. V. Kucherov, L. M. Kustov, M. L. Gening and N. E. Nifantiev, *Mendeleev Commun.*, 2015, **25**, 75.
8 M. D. Mashkovskii, *Lekarstvennye sredstva (Drugs)*, 15th edn., Novaya volna, Moscow, 2005 (in Russian).
9 H. D. Rudolph, J. Demaison and A. G. Császár, *J. Phys. Chem. A*, 2013, **117**, 12969.
10 C. Puzzarini, *Int. J. Quantum Chem.*, 2016, **116**, 1513.
11 R. A. Kendall, T. H. Dunning, Jr. and R. J. Harrison, *J. Chem. Phys.*, 1992, **96**, 6796.
12 L. Margulès, J. Demaison and J. E. Boggs, *Struct. Chem.*, 2000, **11**, 145.
13 J. Demaison, M. Herman and J. Lievin, *Int. Rev. Phys. Chem.*, 2007, **26**, 391.
14 A. V. Belyakov, V. A. Losev, A. N. Rykov, I. F. Shishkov, V. V. Kuznetsov, A. V. Khakhalev and A. B. Sheremetev, *J. Mol. Struct.*, 2022, **1250**, 131669.
15 A. V. Belyakov, A. A. Oskorbin, V. A. Losev, A. N. Rykov, I. F. Shishkov, L. L. Fershtat, A. A. Larin, V. V. Kuznetsov and N. N. Makhova, *J. Mol. Struct.*, 2020, **1222**, 128856.
16 A. V. Belyakov, K. O. Nikolaenko, A. A. Oskorbin, N. Vogt, A. N. Rykov and I. F. Shishkov, *Mol. Phys.*, 2019, **117**, 1850.
17 E. P. Altova, A. N. Rykov, N. Vogt and I. F. Shishkov, *Mendeleev Commun.*, 2021, **31**, 81.
18 M. J. Frisch, G. W. Trucks, H. B. Schlegel, G. E. Scuseria, M. A. Robb, J. R. Cheeseman, G. Scalmani, V. Barone, G. A. Petersson, H. Nakatsuji, X. Li, M. Caricato, A. V. Marenich, J. Bloino, B. G. Janesko, R. Gomperts, B. Mennucci, H. P. Hratchian, J. V. Ortiz, A. F. Izmaylov, J. L. Sonnenberg, D. Williams-Young, F. Ding, F. Lipparini, F. Egidi, J. Goings, B. Peng, A. Petrone, T. Henderson, D. Ranasinghe, V. G. Zakrzewski, J. Gao,

N. Rega, G. Zheng, W. Liang, M. Hada, M. Ehara, K. Toyota, R. Fukuda, J. Hasegawa, M. Ishida, T. Nakajima, Y. Honda, O. Kitao, H. Nakai, T. Vreven, K. Throssell, J. A. Montgomery, Jr., J. E. Peralta, F. Ogliaro, M. J. Bearpark, J. J. Heyd, E. N. Brothers, K. N. Kudin, V. N. Staroverov, T. A. Keith, R. Kobayashi, J. Normand, K. Raghavachari, A. P. Rendell, J. C. Burant, S. S. Iyengar, J. Tomasi, M. Cossi, J. M Millam, M. Klene, C. Adamo, R. Cammi, J. W. Ochterski, R. L. Martin, K. Morokuma, O. Farkas, J. B. Foresman and D. J. Fox, *Gaussian 16*, *Revision C.01*, Gaussian, Inc., Wallingford, CT, 2016.

19 J. F. Stanton, J. Gauss, L. Cheng, M. E. Harding, D. A. Matthews, P. G. Szalay, A. Asthana, A. A. Auer, R. J. Bartlett, U. Benedikt, C. Berger, D. E. Bernholdt, S. Blaschke, Y. J. Bomble, S. Burger, O. Christiansen, D. Datta, F. Engel, R. Faber, J. Greiner, M. Heckert, O. Heun, M. Hilgenberg, C. Huber, T.-C. Jagau, D. Jonsson, J. Jusélius, T. Kirsch, M.-P. Kitsaras, K. Klein, G. M. Kopper, W. J. Lauderdale, F. Lipparini, J. Liu, T. Metzroth, L. A. Mück, T. Nottoli, D. P. O'Neill, J. Oswald, D. R. Price, E. Prochnow, C. Puzzarini, K. Ruud, F. Schiffmann, W. Schwalbach, C. Simmons, S. Stopkowicz, A. Tajti, J. Vázquez, F. Wang, J. D. Watts, C. Zhang, X. Zheng, J. Almlöf, P. R. Taylor, T. Helgaker, H. J. Aa. Jensen, P. Jørgensen, J. Olsen, A. V. Mitin and C. van Wüllen, *CFOUR V2.00beta*, *a quantum chemical program package*, 2014, http://www.cfour.de.

20 V. A. Sipachev, *J. Mol. Struct.: THEOCHEM*, 1985, **121**, 143.

21 V. A. Sipachev, in *Advances in Molecular Structure Research*, eds. M. Hargittai and I. Hargittai, JAI Press, New York, 1999, vol. 5, pp. 263–311.

22 V. A. Sipachev, *J. Mol. Struct.*, 2001, **567**–**568**, 67.

23 V. A. Sipachev, *Struct. Chem.*, 2000, **11**, 167.

24 B. Andersen, H. M. Seip, T. G. Strand and R. Stølevik, *Acta Chem. Scand.*, 1969, **23**, 3224.

25 C. Peng, P. Y. Ayala, H. B. Schlegel and M. J. Frisch, *J. Comput. Chem.*, 1996, **17**, 49.

26 C. Peng and H. B. Schlegel, *Isr. J. Chem.*, 1993, **33**, 449.

27 A. B. Charette, C. Legault and F. Bélanger-Gariépy, *Acta Crystallogr., Sect. E: Struct. Rep. Online*, 2004, **60**, o1921.

28 A. A. Granovsky, *Firefly computational chemistry program, version 8.2.0*, http://classic.chem.msu.su/gran/gamess/index.html.

29 *Chemcraft – graphical software for visualization of quantum chemistry computations, version 1.8*, https://www.chemcraftprog.com.

Received: 10th April 2023; Com. 23/7144